The Role of Surface Friction in Tropical Intraseasonal Oscillation

WINSTON C. CHAO

NASA Goddard Space Flight Center, Greenbelt, Maryland

BAODE CHEN

Universities Space Research Association, Seabrook, Maryland

(Manuscript received 26 November 1999, in final form 22 August 2000)

ABSTRACT

The role of surface friction in the tropical intraseasonal oscillation, or the Madden–Julian oscillation (MJO), is investigated by comparing two 4-yr integrations with the Goddard atmospheric general circulation model: one with the original model design with one added feature to enhance the intensity of the MJO and the other is identical but with surface friction in the Tropics replaced by its zonal mean value. This comparison indicates that in the second experiment the MJO not only still exists but also exists with similar intensity. The oft-cited frictional wave-CISK (FWC) interpretation for the origin of the MJO, which emphasizes the role of frictionally induced convergence in the surface layer, is reassessed in light of these experiments. The possibility of the MJO in the second experiment being forced by the middle latitudes is excluded by a third experiment. These experiments do not support one of the central ideas in FWC that surface friction plays an instability-enhancing role.

1. Introduction

The Madden–Julian oscillation (MJO), or the tropical intraseasonal oscillation, has attracted much attention, ever since its discovery in the early 1970s (Madden and Julian 1971, 1972, 1994) for reasons of both scientific interest and practical forecasts (Ferranti et al. 1990). Among the theoretical interpretations of the MJO, the wave-CISK (conditional instability of the second kind) mechanism (Chao 1987; Lau and Peng 1987; Miyahara 1987; Hendon 1988; Chang and Lim 1988; Wang 1988; Kirtman and Vernekar 1993; Blade and Hartmann 1993, among many others) is the most popular. The basic assertion of the wave-CISK interpretation is that the cooperation between the low-level convergence associated with the eastward moving Kelvin wave and the cumulus convection generates an eastward moving Kelvin-wave-like mode. Later it was recognized that the MJO has an important Rossby-wave-like component (Chao 1987; Nogues-Paegle et al. 1989). However linear analysis and numerical simulations based on it (even when conditional heating is used) revealed two problems with the wave-CISK interpretation, that is, excessive speed and the most preferred scale being zero or grid scale. Chao (1995) presented a discussion of these problems and attributed them to the particular type of expression for the cumulus heating (the so-called wave-CISK type of heating formulation) used in the linear analyses and numerical studies (i.e., the convective heating is proportional to low-level convergence and a fixed vertical heating profile). It should be pointed out that in the relatively successful simulations of MJO with general circulation models (Slingo et al. 1996; Sperber et al. 1997), the cumulus parameterization is based on convective instability rather than CISK type of heating where convective heating depends on low-level convergence.

Various attempts have been mounted to salvage the wave-CISK interpretation. Among them are the phase-lagged wave-CISK and the frictional wave-CISK (hereafter, FWC). Phase-lagged wave-CISK (Davies 1979), by keeping the so-called wave-CISK type of heating but specifying a lag between convection and low-level convergence, managed to avoid the zero preferred scale problem, but the excessive speed problem remained. Also it created a new problem of not maintaining the close balance between convective heating and adiabatic cooling due to vertical motion (Davies 1979), not to mention the unresolved problem of how to determine theoretically the magnitude of the phase lag. Because of these problems the phase-lagged wave-CISK interpretation is not considered as a strong contender. Chao and Deng (1997) gave further discussion on this matter. FWC (e.g., Wang 1988; Xie and Kubokawa 1990) emphasizes the importance of the low-level frictionally induced convergence that occurs to the east of the con-

Corresponding author address: Dr. Winston C. Chao, Mail Code 913, NASA Goddard Space Flight Center, Greenbelt, MD 20771.
E-mail: Winston.Chao@gsfc.nasa.gov

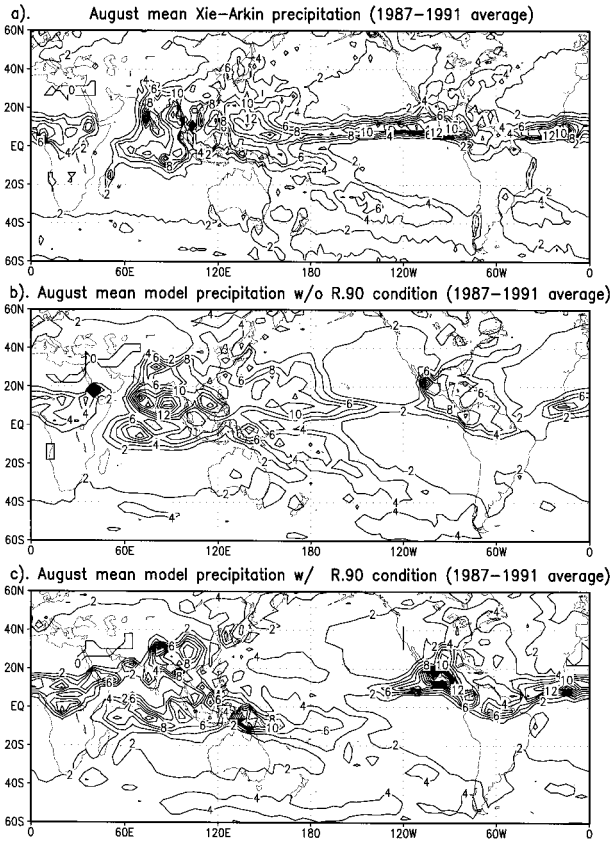

FIG. 1. Four-year (1987–91) averaged precipitation (in mm day $^{-1}$) in Aug for (a) Xie–Arkin observations, and the experiment where the boundary relative humidity condition (b) is not and (c) is imposed.

vective region (thus the eastward movement) (Wang and Rui 1990; Salby et al. 1994; Seager and Zebiak 1994; Wang and Li 1994; Maloney and Hartmann 1998). It also managed to avoid the problem of zero preferred scale. But the excessive speed problem is not completely resolved at least in the linear analysis, though it is possible that when a different convective scheme is used this problem may disappear. The FWC interpretation has gained some notice in recent years (e.g., Salby et al. 1994; Sperber et al. 1997), especially after rasearchers encountered difficulties with another important contending interpretation—the wind-induced surface heat exchange (WISHE) mechanism (Emanuel 1987; Neelin et al. 1987). WISHE requires the surface heat fluxes to be larger to the east of the convective region (so as to induce the convection region to move eastward) than to the west. Recent observational studies have shown that this is not the case (e.g., Chen et al. 1996; Lin and Johnson 1996). For a more thorough review of the theories of the MJO see Hayashi and Golder (1993) and for a more complete citation of the MJO literature see Hayashi and Golder (1997).

The increasing attention that the FWC interpretation of the MJO has received motivated us to investigate the role of the surface friction in the MJO by comparing two integrations of a GCM. The first experiment (referred to as control or CNTL) is a 4-yr integration using the original GCM with one additional feature to enhance the intensity of the MJO. The second experiment (referred to as experiment 1 or EXP1) is identical to CNTL in all aspects except that the surface friction in the Tropics (30°S–30°N) is replaced by its zonal mean value. Since the FWC mechanism is supposed to operate in the Tropics, the replacement of surface friction is done only in the Tropics in EXP1. Also since the FWC mechanism is supposed to act on the wave components, zonal mean surface friction is retained. CNTL is demonstrated to exhibit an MJO signal; thus, the model is considered suitable for the present purpose. However the model has weaknesses that are common to most GCMs (Slingo et al. 1996); that is, that the simulated MJO intensity is not as high as the observed, its period is 30 days[1] versus the observed 30–60 days, and the seasonal change in its intensity is unrealistic. Then, EXP1 is demonstrated to exhibit MJO with nearly the same amplitude, thus indicating that frictional wave-CISK mechanism is not necessary to the existence of the MJO. Our conclusion is that surface friction plays only a modifying role in MJO. This implies that the instability-enhancing role of surface friction that FWC interpretation of the MJO envisions should be discounted. The possibility of the MJO in EXP1 being forced by the middle latitudes is excluded in a third experiment (EXP2) where the meridional wind poleward of 30°N and 30°S is set to zero after every dynamics step in addition to what is done in EXP1. These experiments present no contradiction to our MJO theoretical framework, which was presented in Chao and Lin (1994) and Chao and Deng (1998).

2. The model

The latest version of the Goddard Earth Observing System general circulation model version 2 (GEOS-2) is used. A 4° (latitude) × 5° (longitude) grid size and 20 levels are used. This model uses the discrete dynamics of Suarez and Takacs (1995). The relaxed Arakawa–Schubert scheme (RAS; Moorthi and Suarez 1992) is a main feature of the model. This scheme gives almost identical time mean results as the original Arakawa–Schubert scheme at much reduced computational cost. A condition that the relative humidity of the boundary layer has to be greater than 90% for the cumulus convective to occur, following Wang and Schlesinger (1999), is imposed. Without this condition the MJO still

[1] As noted in Chao (1995), this 30-day period is not the same as the 30-day period obtained in the wave-CISK linear analysis or simulation based on wave-CISK in the sense that the convection associated with the MJO in our model moves in 30 days only the distance of a third of the globe, from eastern Africa to the date line, whereas the convection in the wave-CISK studies moves in 30 days the entire equatorial belt. Some wave-CISK studies obtained an even shorter period.

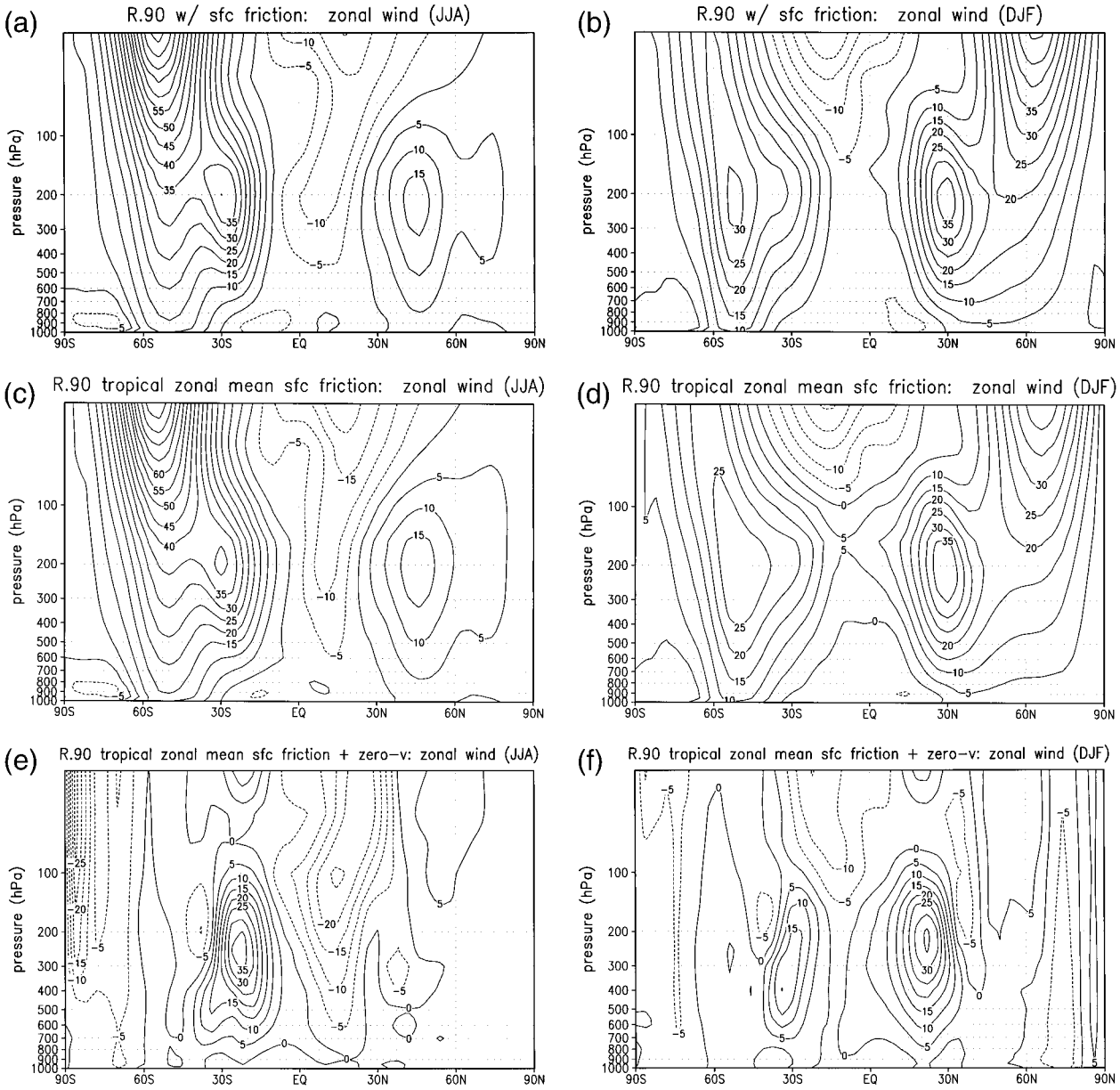

FIG. 2. The DJF and JJA 4-yr mean of zonally averaged zonal wind (in m s^{-1}) for (a, b) CNTL, (c, d) EXP1, (e, f) EXP2.

exists but is weaker. RAS is used in conjunction with a rain–reevaporation scheme (Sud and Molod 1988). The large-scale moist and dry convection remain the same as documented in Kalnay et al. (1983). The boundary layer and turbulence parameterization, a level-2.5 second-order closure model, is that of Helfand and Labraga (1988, 1989). The gravity wave drag parameterization is that of Zhou et al. (1996). The longwave radiation package is that of Chou and Suarez (1994). The shortwave radiation package is that of Chou (1992) and Chou and Lee (1996). The prognostic cloud water parameterization of Del Genio et al. (1996) is used. The land surface process parameterization is that of Koster and Suarez (1996). Sea surface temperature, sea ice, and snow are from observations (for details, see Takacs et al. 1994).

As an aside, we would like to point out that the condition of boundary layer relative humidity being larger than 90% (r.90 condition), though helpful in simulating the MJO, has drawbacks. Our experiments show that such a condition creates a large distortion in the precipitation pattern (and the associated circulation pattern). Figure 1 shows a comparison of the August mean precipitation of climatology, CNTL, and EXP1 for the integration period of 1987–91 with observed surface conditions. The results with the r.90 condition show the

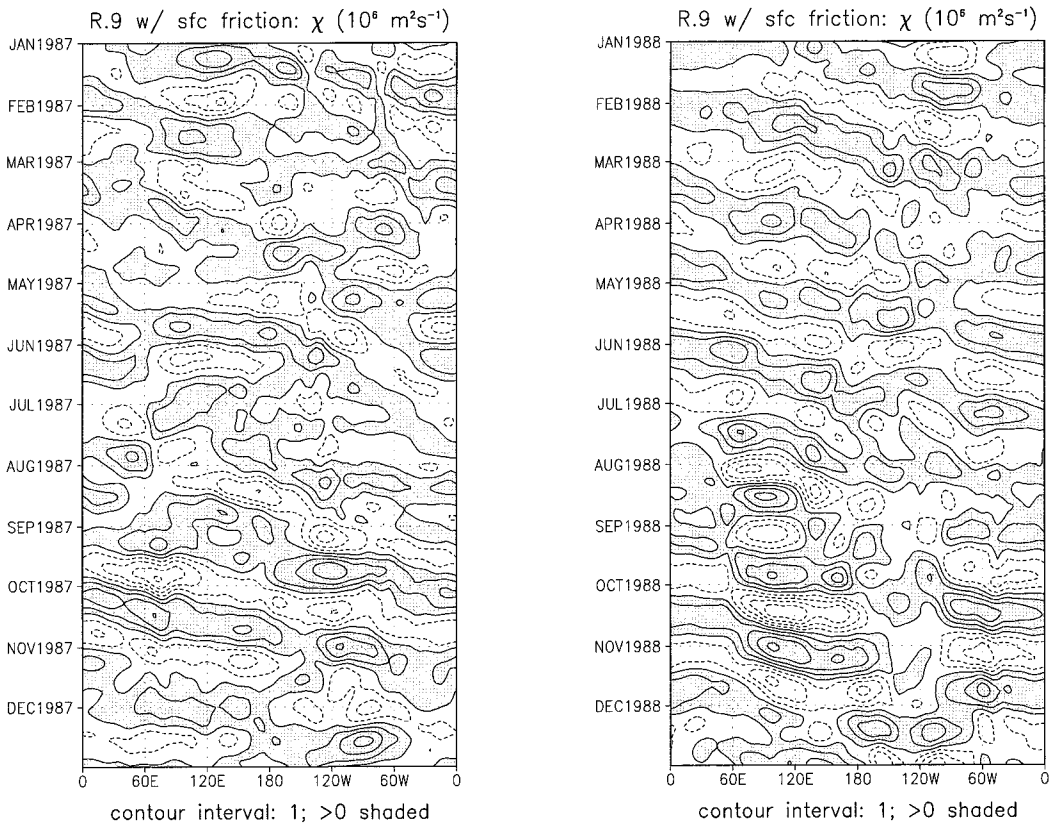

FIG. 3. The 200-hPa velocity potential (in 10^{-6} m^2 s^{-1}) at 2°N as a function of time and longitude for 1987 and 1988 in CNTL. The first solid line is the zero line.

absence of a dry region in the western Indian Ocean, excessive minimum in precipitation around 8°N in the Indian Ocean and around 10°N in the western Pacific, and excessive precipitation over Central America, features not found in the observation or in the experiment without the r.90 condition.

3. Results and discussions

Both CNTL and EXP1 started from 1 January 1987 with the ECMWF reanalysis data as the initial conditions and ran for 4 yr. The results are summarized as follows.

a. Zonal mean wind fields

In the 4-yr average of both the December–January–February (DJF) and the June–July–August (JJA) zonal mean zonal wind fields of the two experiments are shown in Fig. 2. Poleward of 30° the difference between the two experiments is rather unremarkable, though the summer upper-tropospheric jet in DJF is somewhat weaker in EXP1 than in CNTL. In the Tropics the differences between the two experiments are substantial. The zero line in the Southern Hemisphere in JJA moves closer to the equator in EXP1. In DJF a substantial part of tropical upper troposphere is occupied by westerlies in EXP1. The zonally averaged meridional wind fields (not shown) show that the Hadley circulation is slightly stronger and extends a little higher in EXP1 than CNTL in both the DJF and JJA seasons.

b. 200-hPa velocity potential

The 200-hPa velocity potential is equivalent to divergence at that level, which is closely related to precipitation, divided by the total wavenumber squared. Thus the low zonal wavenumbers and low meridional modes are heavily weighted. Therefore this field is particularly suitable for detecting the intraseasonal signal, which has a planetary scale. The variance of this field in the 30–60-day band is concentrated in the Indian Ocean and western Pacific in both integrations. Figure 3 shows band-passed 200-hPa velocity potential along the equator as a function of time in 1987 and 1988 for CNTL (the other two years have similar results and are not shown). It is apparent that the model exhibits eastward propagation of the circulation field in the intraseasonal timescale. The signal is clearer in the second half of the year in the Indian Ocean and western Pacific as opposed to January and February in the observation. However, in 1989 and 1990 the stronger intraseasonal

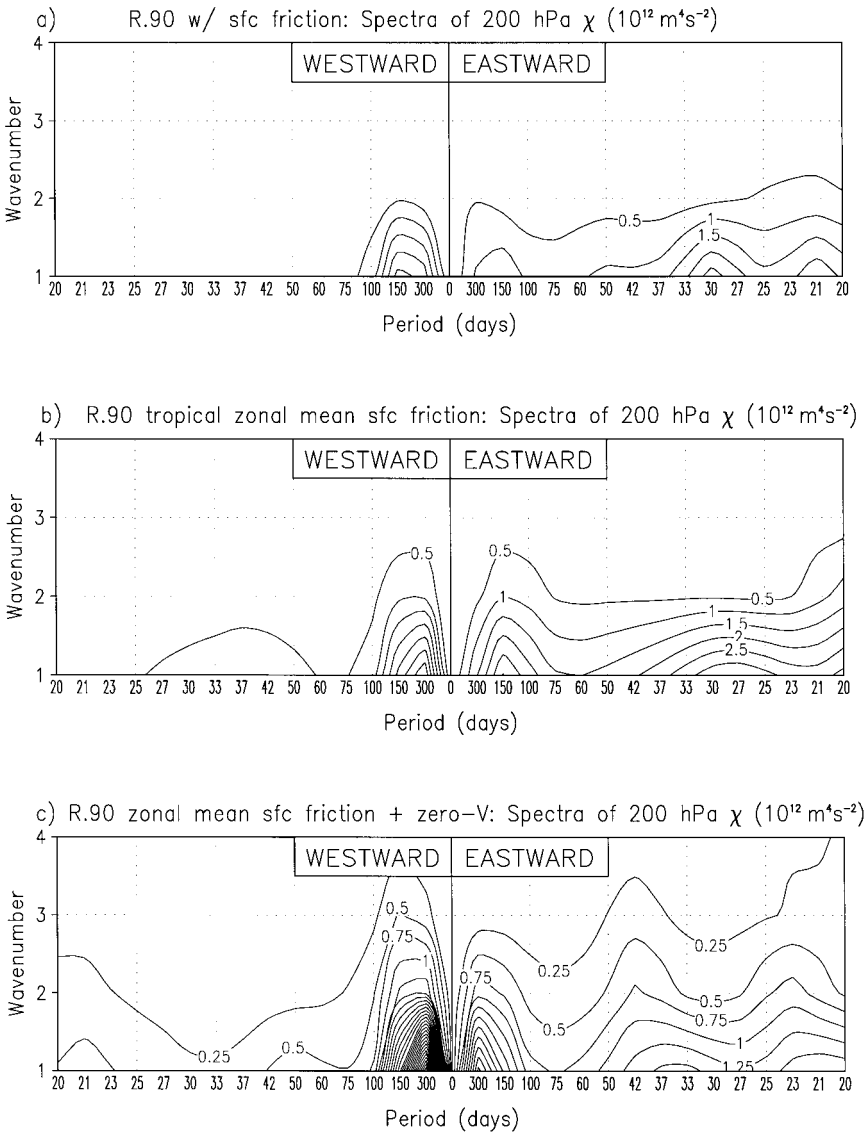

FIG. 4. Power spectra of the 200-hPa velocity potential (in 10^{-12} m^4 s^{-2}) at 2°N in (a) CNTL, (b) EXP1, and (c) EXP2.

signal occurs in northern winter. Thus the model results do not show good seasonal dependence of the intraseasonal signal. The same plots for EXP1 (not shown) demonstrate that the tropical intraseasonal oscillation signal exists with roughly the same intensity. The stronger intraseasonal signal in EXP1 does not have a preferred season either.

c. Power spectral analysis

Figures 4a and 4b show the wave-frequency spectrum of the 200-hPa velocity potential at 2°N of the two experiments. There is a clear peak at eastward wavenumber 1 around the 30-day period in CNTL. EXP1 shows a little higher intensity around the 28-day period.

d. Composites

The composites of divergence and vorticity (both in 10^{-7} s^{-1}) based on bandpass- (30–60 days) filtered winds overlapping with precipitation (in mm day^{-1}) are done along the eastward moving precipitation centers in the Indian Ocean and western Pacific as revealed in the bandpass-filtered precipitation field. Figures 5a–f and 5g–l show the results for CNTL and EXP1, respectively. The shaded region is the center of precipitation. These figures clearly show that the intensity of the convection and the associated divergence are slightly greater in EXP1. The precipitation pattern shows protrusions in the WNW and WSW directions for EXP1 (Figs. 5g–l), as is observed [Hendon and Salby (1994,

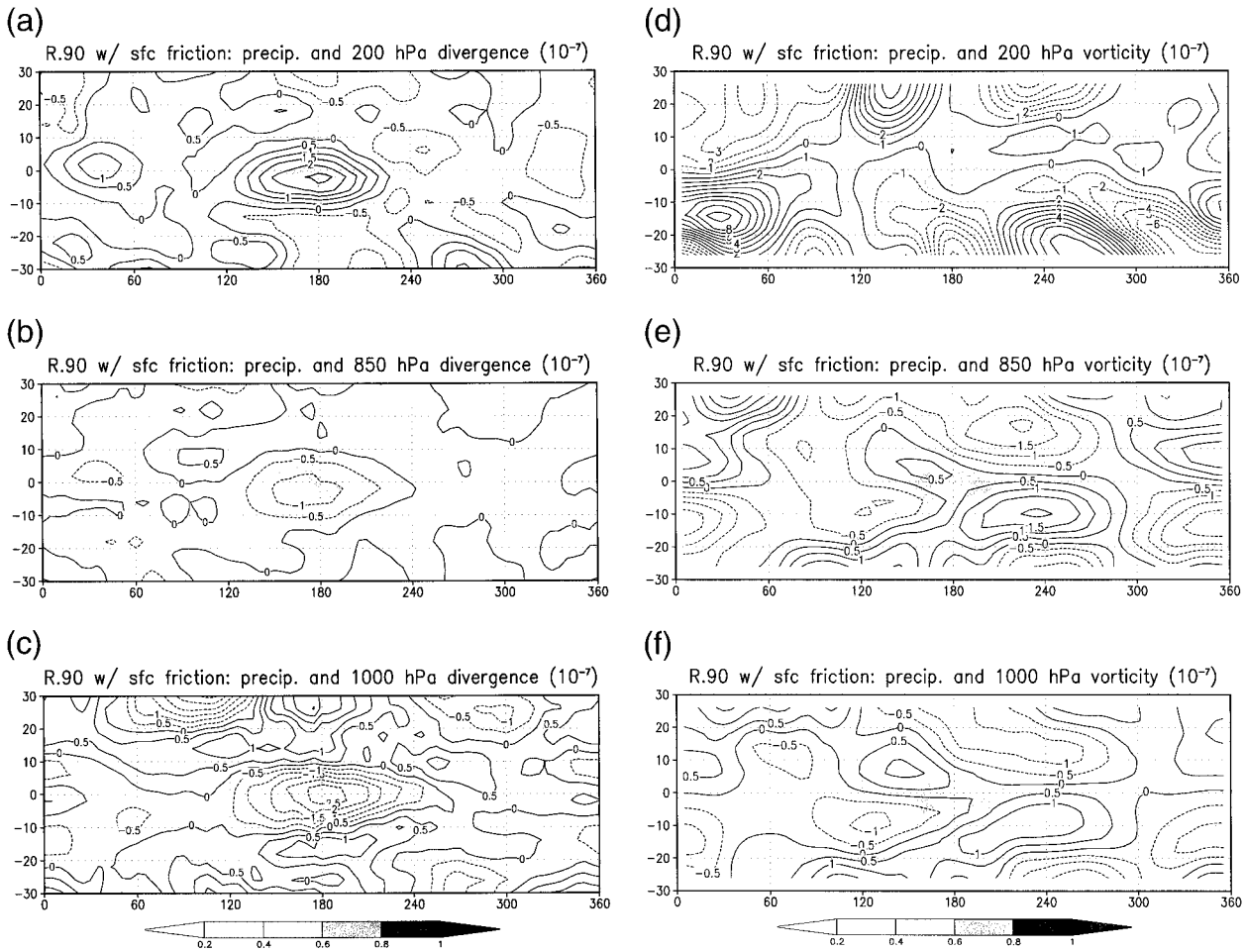

FIG. 5. Composites of the MJO convective regions in terms of precipitation (shaded, in mm day^{-1}), divergence, and vorticity (in 10^{-7} s^{-1} at 200, 850 and 1000 hPa for (a)–(f) CNTL, (g)–(l) EXP1, and (m)–(r) EXP2.

their Fig. 4a), the OLR], but which is not as obvious in CNTL (Figs. 5a–f). At 1000 hPa the convergence field is centered slightly to the east of the precipitation center in both experiments. The 1000-hPa vorticity composites of both experiments show vorticity centers to the northwest and southwest of the precipitation (or the low-level convergence). This is a signature of a coupled Rossby and Kelvin wave–like mode. Therefore the intraseasonal disturbances in the model are indeed an MJO mode rather than a Kelvin wave–like mode. Notice that precipitation occurs at the nodal lines of the 1000-hPa vorticity in both CNTL and EXP1.

To summarize, our results do not support the FWC interpretation of the MJO. This calls for the abandonment of the FWC interpretation of the MJO, which emphasizes the low-level convergence induced by surface friction. Our experimental results are consistent with the idea expounded by Emanuel et al. (1994) and Raymond (1995) that low-level convergence is the result rather the cause of convection (at least on timescales greater than one-half of a day). Their idea implies that surface friction does not induce low-level convergence. If surface friction could induce low-level convergence, then low-level convergence would have to generate convection in contradiction to their idea. In other words, our experiments do not support the dual role of surface friction as described by Charney and Eliassen (1964) in their CISK theory. Equivalently, our experiments support the notion that surface friction plays only one role in the MJO: damping.

One might be curious about the possibility that the MJO in EXP1 may be due to middle-latitude forcing in the absence of the FWC mechanism. This possibility can be excluded by a third experiment (EXP2), in which EXP1 is repeated with the meridional wind poleward of 30°N and 30°S set to zero after every dynamics time step. The results of EXP2 (Figs. 2e, 2f, 4c, and 5m–r) show that the MJO still exists, despite the large difference in the tropical zonal mean wind field and the weaker MJO amplitude and longer period (34 days in EXP2 vs 28 days in EXP1; Fig. 4.c) in EXP2. Thus, we can conclude that the MJO in EXP1 is of tropical origin.

Thus far we do not yet have a comprehensive interpretation for the origin of the MJO and finding it will

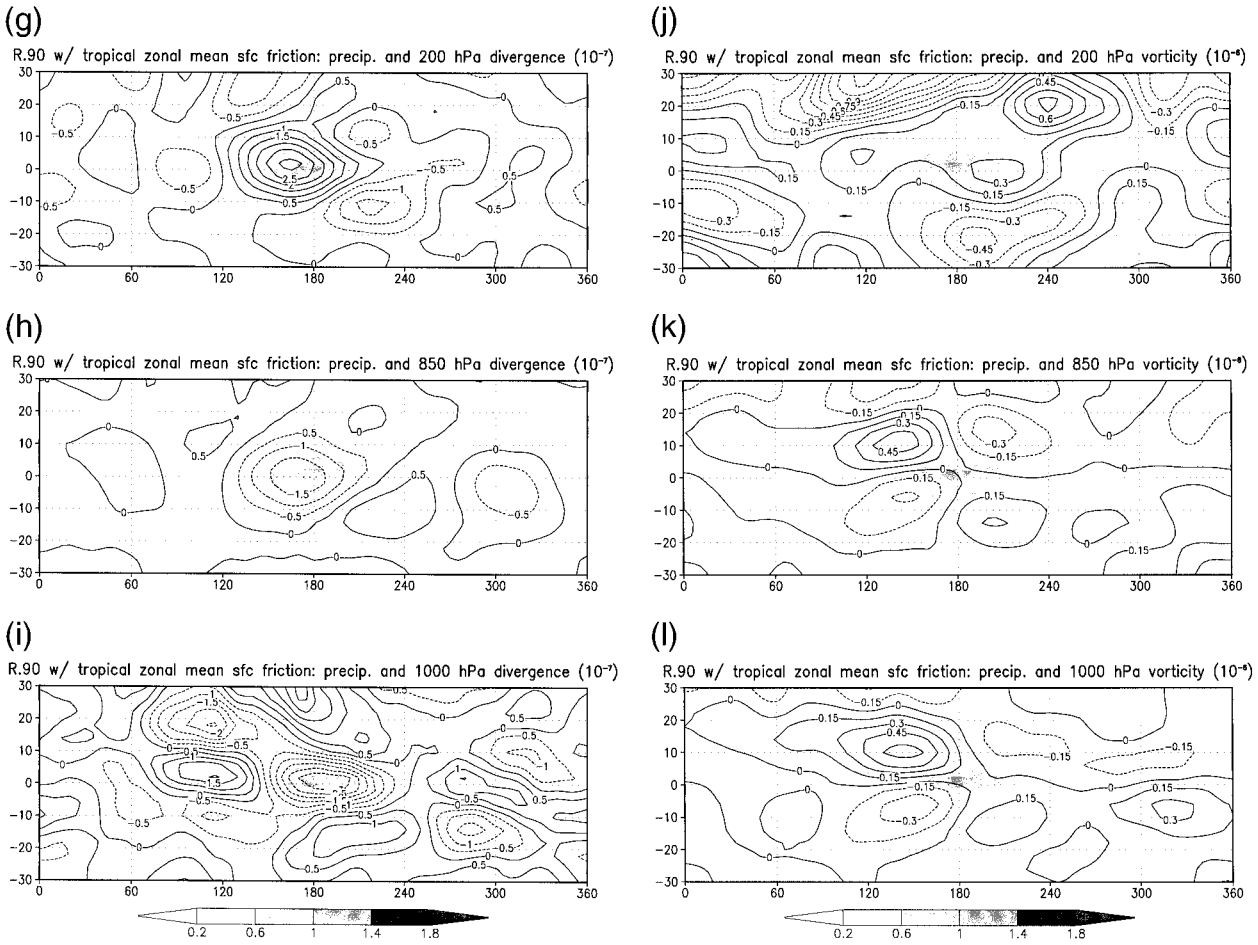

FIG. 5. (*Continued*)

be our future objective. Currently we are pursuing in a direction based on the idea of the MJO being driven by wave packet (or soliton)–like super–cloud clusters (Chao and Lin 1994; Chao and Deng 1998).

Acknowledgments. The late Yoshio Hayashi of GFDL and an anonymous reviewer provided useful suggestions. This work was supported by the NASA Earth Science Division with funds managed by Kenneth Bergman.

REFERENCES

Blade, I., and D. L. Hartmann, 1993: Tropical intraseasonal oscillations in a simple nonlinear model. *J. Atmos. Sci.,* **50,** 2922–2939.

Chang, C.-P., and H. Lim, 1988: Kelvin wave-CISK: A possible mechanism for the 30–50 day oscillations. *J. Atmos. Sci.,* **45,** 1709–1720.

Chao, W. C., 1987: On the origin of the tropical intraseasonal oscillation. *J. Atmos. Sci.,* **44,** 1940–1949.

——, 1995: A critique of wave-CISK as the explanation for the 40–50 day tropical intraseasonal oscillation. *J. Meteor. Soc. Japan,* **73,** 677–684.

——, and S.-J. Lin, 1994: Intraseasonal oscillation, super cloud clusters, and cumulus convection schemes. *J. Atmos. Sci.,* **51,** 1282–1297.

——, and L. Deng, 1997: Phase lag between deep cumulus convection and low-level convergence in tropical synoptic systems. *Mon. Wea. Rev.,* **125,** 549–559.

——, and ——, 1998: Tropical intraseasonal oscillation, super cloud clusters, and cumulus convection schemes. Part II: 3D aqua-planet simulations. *J. Atmos. Sci.,* **55,** 690–709.

Charney, J. G., and A. Eliassen, 1964: On the growth of the hurricane depression. *J. Atmos. Sci.,* **21,** 68–75.

Chen, S. S., R. A. Houze, and B. E. Mapes, 1996: Multiscale variability of deep convection in relation to large-scale circulation in TOGA COARE. *J. Atmos. Sci.,* **53,** 1380–1409.

Chou, M. D., 1992: A solar-radiation model for use in climate studies. *J. Atmos. Sci.,* **49,** 762–722.

——, and M. J. Suarez, 1994: An efficient thermal infrared radiation parameterization for use in general circulation models. NASA Tech. Memo. 104606, Vol. 3, 85 pp.

——, and K.-T. Lee, 1996: Parameterizations for the absorption of solar radiation by water vapor and ozone. *J. Atmos. Sci.,* **53,** 1203–1208.

Davies, H. C., 1979: Phase-lagged wave-CISK. *Quart. J. Roy. Meteor. Soc.,* **105,** 325–353.

Del Genio, A. D., M.-S. Yao, W. Kovari, and K. K.-W. Lo, 1996: A prognostic cloud water parameterization for general circulation models. *J. Climate,* **9,** 270–304.

Emanuel, K. A., 1987: An air–sea interaction model of intraseasonal oscillation in the tropics. *J. Atmos. Sci.,* **44,** 2324–2340.

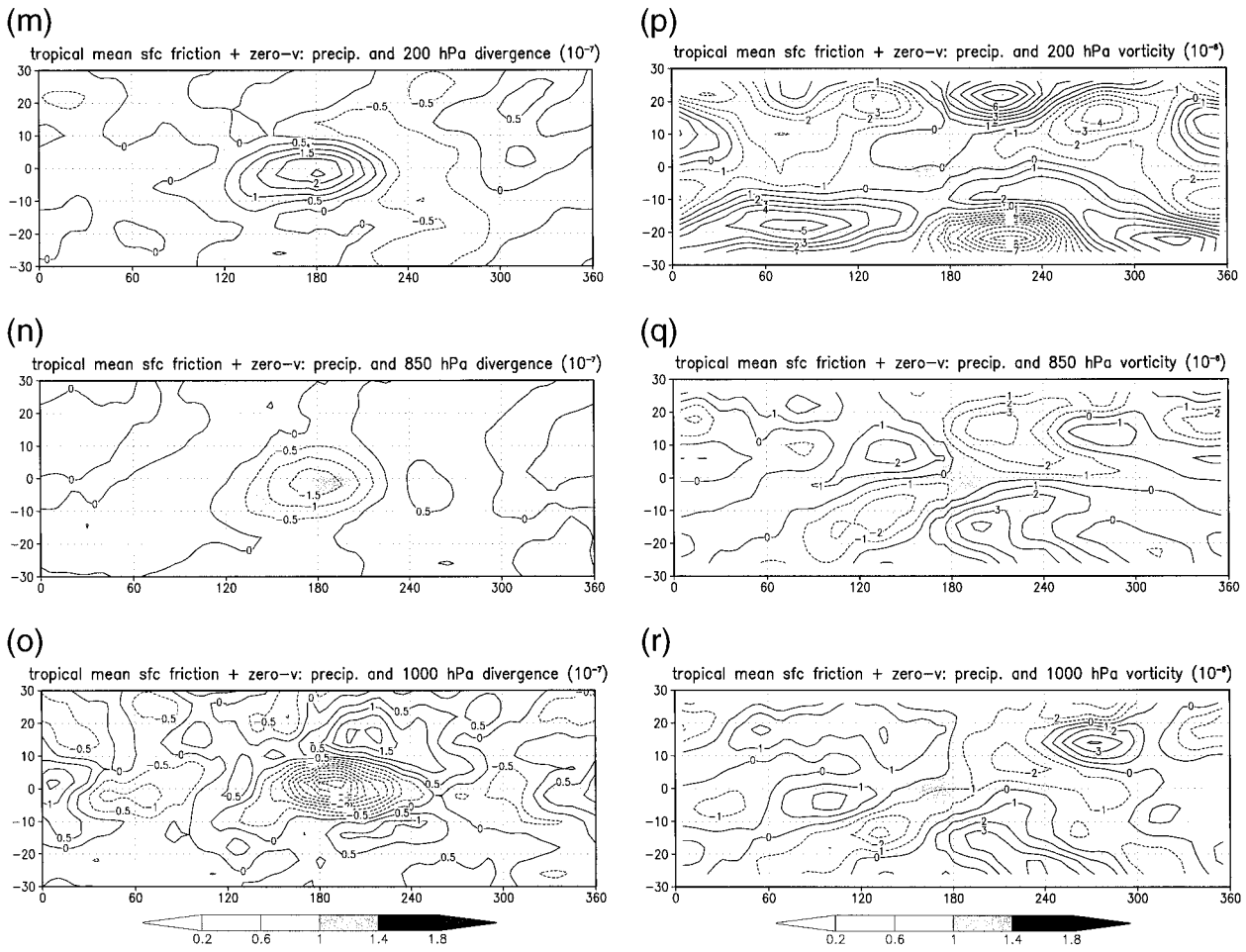

FIG. 5. (*Continued*)

——, J. D. Neelin, and C. S. Bretherton, 1994: On large-scale circulations in convecting atmosphere. *Quart. J. Roy. Meteor Soc.*, **120,** 1111–1145.

Ferranti, L., T. N. Palmer, F. Molteni, and E. Klinker, 1990: Tropical–extratropical interaction associated with the 30–60 day oscillation and its impact on medium and extended range prediction. *J. Atmos. Sci.,* **47,** 2177–2199.

Hayashi, Y., and D. G. Golder, 1993: Tropical 40–50 and 25–30 day oscillations appear in realistic and idealized GFDL climate models and the ECMWF database. *J. Atmos. Sci.,* **50,** 464–494.

——, and ——, 1997: United mechanisms for the generation of low- and high-frequency tropical waves. Part I: Control experiments with moist convective adjustment. *J. Atmos. Sci.*, **54,** 1262–1276.

Helfand, H. M., and J. C. Labraga, 1988: Design of a non-singular level 2.5 second-order closure model for the prediction of atmospheric turbulence. *J. Atmos. Sci.,* **45,** 113–132.

——, and ——, 1989: Reply. *J. Atmos. Sci.,* **46,** 1633–1635.

Hendon, H. H., 1988: A simple model of the 40–50 day oscillation. *J. Atmos. Sci.*, **45,** 569–584.

——, and M. L. Salby, 1994: The life cycle of the Madden–Julian oscillation. *J. Atmos. Sci.,* **51,** 2225–2237.

Kalnay, E., R. Balgovind, W. Chao, D. Edelmann, J. Pfaendtner, L. Takacs, and K. Takano, 1983: Documentation of the GLAS fourth-order general circulation model. Vol. 1: Model description. NASA Tech Memo. 86064. [Available from Library, NASA Goddard Space Flight Center, Greenbelt, MD 20771.]

Kirtman, B., and A. Vernekar, 1993: On wave-CISK and the evaporation–wind feedback for the Madden–Julian oscillation. *J. Atmos. Sci.,* **50,** 2811–1814.

Koster, R., and M. Suarez, 1996: Energy and water balance calculations in the Mosaic LSM. NASA Tech. Memo. 104606, Vol. 9, 60 pp. [Available from Library, NASA Goddard Space Flight Center, Greenbelt, MD 20771.]

Lau, K.-M., and L. Peng, 1987: Origin of low-frequency (intraseasonal) oscillations in the tropical atmosphere. Part I: Basic theory. *J. Atmos. Sci.,* **44,** 950–972.

Lin, X., and R. H. Johnson, 1996: Kinematic and thermodynamic characteristics of the flow over the western Pacific warm pool during TOGA COARE. *J. Atmos. Sci.,* **53,** 695–715.

Madden, R. A., and P. R. Julian, 1971: Detection of a 40–50 day oscillation in the zonal wind in the tropical Pacific. *J. Atmos. Sci.,* **28,** 702–708.

——, and ——, 1972: Description of global scale circulation cells in the tropics with a 40–50 day period. *J. Atmos. Sci.,* **29,** 1109–1123.

——, and ——, 1994: Observations of the 40–50-day tropical oscillation—A review. *Mon. Wea. Rev.,* **122,** 814–837.

Maloney, E. D., and D. L. Hartmann, 1998: Frictional moisture convergence in a composite life cycle of the Madden–Julian oscillation. *J. Climate,* **11,** 2387–2403.

Miyahara, S., 1987: A simple model of the tropical intraseasonal oscillation. *J. Meteor. Soc. Japan,* **65,** 341–351.

Moorthi, S., and M. J. Suarez, 1992: Relaxed Arakawa–Schubert: A

parameterization of moist convection for general circulation models. *Mon. Wea. Rev.,* **120,** 978–1002.

Neelin, J. D., I. M. Held, and K. H. Cook, 1987: Evaporation–wind feedback and low-frequency variability. *J. Atmos. Sci.,* **44,** 2341–2348.

Nogues-Paegle, J., B.-C. Lee, and V. E. Kousky, 1989: Observed modal characteristics of the intraseasonal oscillation. *J. Climate,* **2,** 496–507.

Raymond, D. J., 1995: Regulation of moist convection over the western Pacific warm pool. *J. Atmos. Sci.,* **52,** 3945–3959.

Salby, M. L., R. R. Garcia, and H. H. Hendon, 1994: Planetary-scale circulations in the presence of climatological and wave-induced heating. *J. Atmos. Sci.,* **51,** 2344–2367.

Seager, R., and S. E. Zebiak, 1994: Convective interaction with dynamics in a linear primitive model. *J. Atmos. Sci.,* **51,** 1307–1331.

Slingo, J. M., and Coauthors, 1996: Intraseasonal oscillations in 15 atmospheric general circulation models: Result from an AMIP diagnostic subproject. *Climate Dyn.,* **12,** 325–358.

Sperber, K. R., J. M. Slingo, P. M. Inness, and W. K.-M. Lau, 1997: On the maintenance and initiation of the intraseasonal oscillation in the NCEP/NCAR reanalysis and the GLA and UKMO AMIP simulations. *Climate Dyn.,* **13,** 769–795.

Suarez, M. J., and L. L. Takacs, 1995: Documentation of the Aries–GEOS dynamical core: Version 2. NASA Tech. Memo. 104606, Vol. 5, 44 pp. [Available from Library, NASA Goddard Space Flight Center, Greenbelt, MD 20771.]

Sud, Y. C., and A. Molod, 1988: The roles of dry convection, cloud-radiation feedback processes and the influence of recent improvements in the parameterization of convection in the GLA GCM. *Mon. Wea. Rev.,* **116,** 2366–2387.

Takacs, L. L., A. Molod, and T. Wang, 1994: Documentation of the Goddard Earth Observing System (GEOS) General Circulation Model—Version 1. NASA Tech. Memo. 104606, Vol. 1, 100 pp. [Available from Library, NASA Goddard Space Flight Center, Greenbelt, MD 20771.]

Wang, B., 1988: Dynamics of tropical low-frequency waves: An analysis of the moist Kelvin wave. *J. Atmos. Sci.,* **45,** 2051–2065.

——, and H. Rui, 1990: Dynamics of the coupled moist Kelvin–Rossby wave on an equatorial beta-plane. *J. Atmos. Sci.,* **47,** 397–413.

——, and T. Li, 1994: Convective interaction with boundary layer dynamics in the development of tropical intraseasonal system. *J. Atmos. Sci.,* **51,** 1386–1400.

Wang, W., and M. E. Schlesinger, 1999: The dependence on convection parameterization of the tropical intraseasonal oscillation simulated by the UIUC 11-layer atmospheric GCM. *J. Climate,* **12,** 1423–1457.

Xie, S.-P., and A. Kubokawa, 1990: On the wave-CISK in the presence of a frictional boundary layer. *J. Meteor. Soc. Japan,* **68,** 651–657.

Zhou, J., Y. C. Sud, and K.-M. Lau, 1996: Impact of orographically induced gravity-wave drag in the GLA GCM. *Quart. J. Roy. Meteor. Soc.,* **122,** 903–927.